


Article

Evaluation and Prediction of Groundwater Quality in the Source Region of the Yellow River

Jianhua Si ^{1,†}, Jianming Li ^{2,†}, Ying Yang ², Xuejiao Qi ², Jiajun Li ², Zenghui Liu ², Mengyuan Li ¹, Sujin Lu ^{2,*} , Yue Qi ², Cheng Jin ², Lijuan Qi ², Bingyu Yi ² and Yujing Wang ²

¹ College of Agriculture and Animal Husbandry, Qinghai University, Xining 810016, China

² Eco-Environmental Engineering College, Qinghai University, Xining 810016, China

* Correspondence: lusujin88@163.com

† These authors contributed equally to this work.

Abstract: With the disturbance of human factors, the groundwater resources in the source region of the Yellow River have gradually depleted and the water quality has become worse, which has seriously affected the development of high-altitude areas. The groundwater quality of the source region of the Yellow River from 2016 to 2020 was evaluated using single-component and comprehensive evaluation methods, following by a prediction of the groundwater quality from 2021 to 2100 based on the RCPS (RCP 2.6, RCP 4.5, and RCP 8.5) scenarios coupled with the SWAT hydrological model under the CMIP5 global climate model. The results indicated that the groundwater temperature had an increasing trend, pH showed an obvious decreasing trend, and total hardness (Th), sulfate, and ammonia nitrogen (NH₄⁺-N) contents exhibited no obvious increasing or decreasing trend in the source region of the Yellow River during 2016–2020. The increase rate of total nitrogen (TN) and total phosphorus (TP) in the future climate scenario followed the order of RCP 8.5 > RCP 4.5 > RCP 2.6, and the groundwater contents of TN and TP in the source region of the Yellow River gradually increased. This result is of great significance, as it can help clarify the current situation of groundwater in high-altitude and cold regions, showing the influence of groundwater on global climate change. It provides a reference for the development and utilization planning of groundwater resources in the source region of the Yellow River in the future.

Keywords: the source region of the Yellow River; groundwater; water quality evaluation and prediction; CMIP5; RCPS; SWAT hydrological mode



Citation: Si, J.; Li, J.; Yang, Y.; Qi, X.; Li, J.; Liu, Z.; Li, M.; Lu, S.; Qi, Y.; Jin, C.; et al. Evaluation and Prediction of Groundwater Quality in the Source Region of the Yellow River. *Water* **2022**, *14*, 3946. <https://doi.org/10.3390/w14233946>

Academic Editor: Domenico Cicchella

Received: 7 November 2022

Accepted: 29 November 2022

Published: 4 December 2022

Publisher's Note: MDPI stays neutral with regard to jurisdictional claims in published maps and institutional affiliations.



Copyright: © 2022 by the authors. Licensee MDPI, Basel, Switzerland. This article is an open access article distributed under the terms and conditions of the Creative Commons Attribution (CC BY) license (<https://creativecommons.org/licenses/by/4.0/>).

1. Introduction

Groundwater is an important resource for the sustainable development of human society, but global groundwater resources are being significantly depleted [1–3]. Groundwater pollution is a difficult problem to solve, and has led to problems in many countries related to water resource utilization, and even serious groundwater resources crises [4]. Some unreasonable and inefficient ways of developing and utilizing groundwater resources have caused the groundwater pollution [5]. Groundwater quality evaluation is an important technical method for groundwater ecological planning and management, and it is a key theoretical basis for groundwater pollution prevention and control [6]. In recent decades, many scholars have proposed a variety of corresponding water quality evaluation methods based on groundwater quality monitoring data. Babiker [7] proposed a GIS-based groundwater quality index (GQI), which selects the best parameters to calculate GQI and incorporates temporal changes to evaluate groundwater quality. Maged [8] assessed groundwater resources using a variety of water quality indexes (WQIs), GIS methods, and partial least squares regression models (PLSR) and used NETPATH and water quality indices to assess the geochemical evolution of groundwater quality near the El Harga Oasis, Egypt [9]. Maryam [10] measured the sodium sorption ratio and conductivity parameters obtained in

384 wells in Iran to determine groundwater quality from 2005 to 2014. Hawzhin et al. [11] predicted groundwater table changes in the Lake Urmia Basin based on Gravity Recovery and Climate Experiment (GRACE) satellite data. Chinese scholars, Aifang Cheng et al. [12], Yingjia Zhai et al. [13], Zhimei Yuan et al. [14], and Julong Deng et al. [15], conducted groundwater response studies from northwest to north China assessing climate change, coupling future climate scenarios with hydrological and water quality models and applying them to groundwater prediction work. Climate models and hydrological models are the main tools used worldwide to examine hydrological and water resources under changing environments [16].

In the IPCC Fifth Assessment Report (AR5) [17], the climate model of the fifth phase of the coupled model comparison plan (CMIP5) and new emission scenarios (typical concentration path RCP, RCP includes RCP2.6, RCP4.5 and RCP8.5) [18] were used to predict future changes in the climate system, which achieved good results [19,20]. Among them, RCP2.6 represent the scenario with the lowest greenhouse gas (mainly CO₂, CH₄, and N₂O) emissions and concentrations [21]. RCP4.5 is a climate change scenario for climate policy intervention [21]. RCP8.5 is a scenario without climate policy intervention to reduce greenhouse gas emissions, where the concentration of greenhouse gas emissions is the highest [22,23]. Based on these GHG concentration scenarios, projections of future global climate and different climate projections will be made for different GHG concentration scenarios. For this, we need to predict the water quality of groundwater in the source region of the Yellow River under different future GHG emission scenarios. SWAT is a long-term, distributed hydrological model that has been extensively used [24]. Meshesha et al. [25] simulated nitrate and total dissolved solid (TDS) parameters in groundwater in the Athabasca River Basin, and concluded that the extended SWAT model could be a powerful tool for regional-scale nutrient loading simulations. Meshesha et al. [26] applied the SWAT basin-scale water quality module to a cold region by improving it to study the effects of the water quality module in the Athabasca River Basin, Alberta, and the effects on water ecosystems and water quality processes were studied to obtain accurate ranges of DO, DOC and FC contents daily. Luo et al. [27] applied the SWAT model to simulate groundwater changes in the Mascatec River basin and obtained better results. Guzman et al. [28] coupled the SWAT model with MODFLOW as a way to simulate groundwater flow changes. Simulation studies have been carried out in China using the SWAT model for the Ring North, the Xilin River, and the upper Yangtze River basin, and continuous improvements have been made to the application of the SWAT model [29–32]. Junye et al. [33] summarized the elements of hydrological models used in alpine regions and concluded that existing watershed models need to be calibrated and validated against observed data, and that an integrated watershed simulation is the key to the sustainable management of soil and water resources in cold regions. SWAT models have become an important tool for predicting groundwater quality at the global scale, and a large number of models have been developed in recent decades, but most modeling has focused on understanding spatial and temporal groundwater storage and flow [34]. The simulation of the distribution of chemical elements in groundwater using SWAT models is weak.

The source region of the Yellow River is located on the Qinghai–Tibet Plateau, the birthplace of the Yellow River. At present, there are few studies on groundwater in the source region of the Yellow River. Zhang Senqi et al. [35] and Wang Jinhua et al. [36] explored the groundwater level in the source region of the Yellow River and predicted the changes in temperature and rainfall but did not evaluate the state of groundwater quality in the source region of the Yellow River and predict the chemical elements in the groundwater under the future climate scenario model. A study using a climate change model coupled with the SWAT hydrological model for future groundwater quality prediction in the source region of the Yellow River has not yet been reported, so using the groundwater quality model as a prediction tool can provide useful insights for mitigating the impact of groundwater non-point source pollution. This study analyzed and evaluated the current groundwater quality situation in the source region of the Yellow River through continuous sampling and

the determination of water quality indicators at seven groundwater monitoring sites from 2016 to 2020, and scientifically described the groundwater quality situation in the source region of the Yellow River. Additionally, we coupled the SWAT hydrological model based on the RCPS (RCP 2.6, RCP 4.5, and RCP 8.5) scenarios under the CMIP5 global climate model to establish the groundwater quality change scenarios from 2021 to 2100 in the source region of the Yellow River and predict the condition of the groundwater quality indicators TN and TP in the source region of the Yellow River. It is of great significance to improve the development and utilization of groundwater resources and create a groundwater resource restoration scheme for the source region of the Yellow River.

2. Materials and Methods

2.1. Location of the Study Area

The Yellow River is known as China's "Mother River". The source region of the Yellow River is the most significant runoff-producing area in the Yellow River. The source region of the Yellow River plays an essential role in the entire Yellow River basin. The geographical location of the region is relatively unique, and the water resources of the region can respond positively to global climate change and serve as a climate regulator for China and even East Asia. The total area of the source region of the Yellow River is about 121,972 km², among which the total length of the main channel reaches 1553 km. The annual average flow is about 20 billion m³, and the water flow in the source region of the Yellow River accounts for about 38% of the whole Yellow River Basin [37]. The source region is in the northeast of the Tibetan Plateau, with a longitude and latitude of 32°09'~36°34' N, 95°54'~103°24' E. The source region belongs to the typical plateau continental climate; the mean sea wave is 4300 m; sunshine hours and radiation are strong; the average temperature is -4.0~5.0 °C. The annual precipitation distribution is uniformed; the average annual precipitation has been between 220 and 780mm for many years; it has a gradual increasing trend from the northwest to southeast region. In recent years, the source region of the Yellow River has been affected by geological processes such as plateau uplift and under-river erosion, resulting in serious fragmentation of water-bearing basins in the source area. The capacity of the entire aquifer to regulate and store water is weakened, resulting in the gradual reduction in groundwater and the deterioration of water quality. The source region of the Yellow River is rich in frozen soil resources, 70.6% of which are covered by permafrost. However, with the development of cities and overgrazing by herdsmen in recent years, as well as global climate change, meadows, wetland and other especially frozen soil resources in this region have degraded to a certain extent. These lead to changes in the underlying surface such as the shrinkage of marshes and the expansion of desertification, contributing to the further degradation of permafrost and the pollution of sewage in the interior of the region. The bedrock strata in this area are mainly Permian, Triassic sandstone, and SLATE intercalated with limestone. The Quaternary strata are mainly composed of ice bonds and ice water facies deposits of the Middle Pleistocene and Upper Pleistocene, and lacustrine strata of the Lower Pleistocene and alluvial, diluvial, aeolian and swamp deposits of the Holocene. Due to the wide distribution of freezing–thawing zones, the permafrost layer plays a role of water isolation. Thereby, the groundwater is mainly divided into water above the frozen layer, water between the frozen layer and water under the frozen layer. The source region of the Yellow River is also a very important protected area in China, with rich biodiversity and ecological functions such as water conservation and climate regulation. If the groundwater quality in the area becomes poor, it will cause the loss of ecosystem service function and further deterioration of the ecological environment. The source region of the Yellow River can be divided into three sub-basins: Tangnai River, Maqu River and Jimaizi River basin. Therefore, seven groundwater-monitoring points representing the groundwater quality of the whole source area have been set up to measure the main runoff of the three sub-basins of the source area. According to the Chinese national standard "Technical Specification for Groundwater Environmental Monitoring" (No. HJ/T 164-2004), from January 2016 to November 2020, shallow groundwater with obvious groundwater

distribution was collected in the dry season, normal season, and wet season every year. Groundwater monitoring points in the source region of the Yellow River are shown in Figure 1 and Table 1.

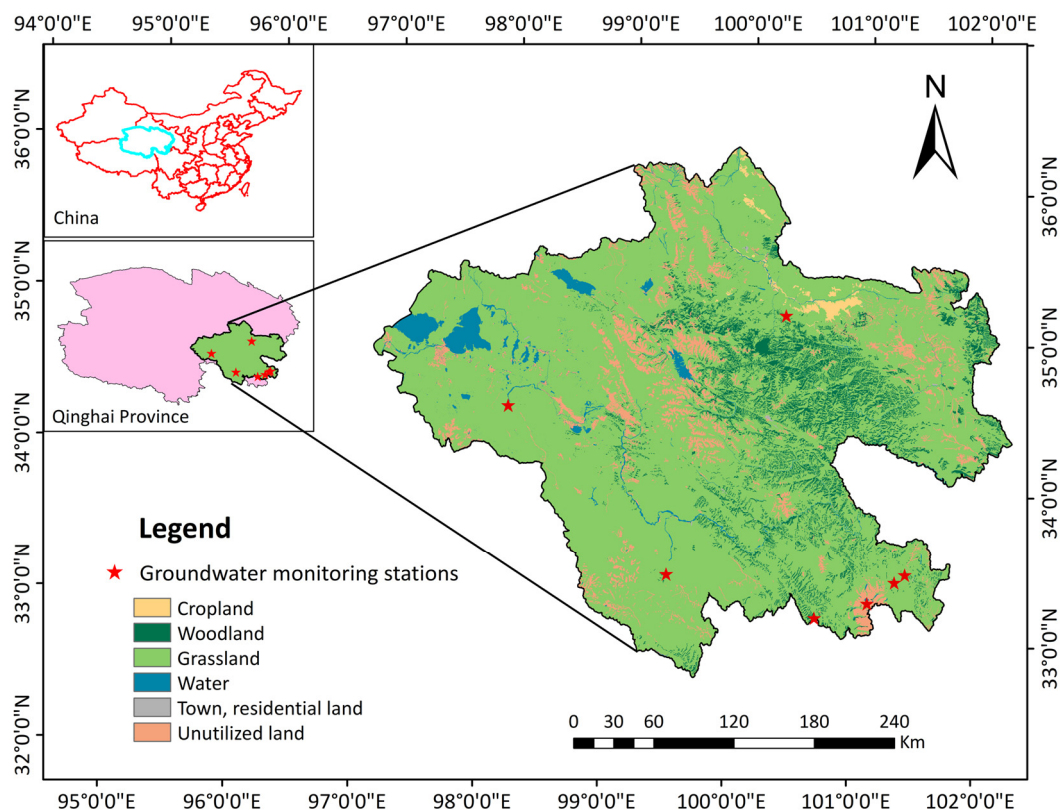


Figure 1. Groundwater monitoring points in the source region of the Yellow River.

Table 1. Location and altitude of groundwater-monitoring points in the source region of the Yellow River.

Serial Number	Observation Point	Longitude	Latitude	Altitude/m
The first monitoring point	The first groundwater area at TongDe junction of 101 provincial highway	100°34.847'	35°15.215'	3233
The second monitoring point	The second groundwater area at TongDe junction of 101 provincial highway	101°41.583'	33°46.097'	3517
The third monitoring point	The first groundwater area at the head of LuanShitou	101°33.200'	33°40.760'	3928
The fourth monitoring point	The second groundwater area at the head of LuanShitou (at 845 km of 101 provincial highway)	101°11.505'	33°26.236'	4045
The fifth monitoring point	The groundwater in LaoDeang township (at 636 km of 101 provincial highway)	100°68.997'	33°15.255'	4173
The sixth monitoring point	The groundwater in WoSai township (the 23 km from DaRi county)	99°46.517'	33°39.595'	4029
The seventh monitoring point	The groundwater in the southern part of Xingxinghai River (at 508 km of 214 National Highway)	98°08.074'	34°45.364'	4283

2.2. Data Collection and Measurement

The selection of groundwater quality indicators was based on the physical and chemical indicators in the Chinese national standard for “groundwater quality standards” (No. GB/T14848-2017), which includes temperature, pH, total hardness (Th), sulfate, oxygen consumption (COD_{Mn}), ammonia nitrogen (NH₄⁺-N), total nitrogen (TN) and total

phosphorus (TP). The temperature and total hardness are some basic physical indicators. Dissolved oxygen, ammonia nitrogen, sulfate, total nitrogen, and total phosphorus were considered as the main pollutants in the source region of the Yellow River. pH was considered because the soils in the area are mainly alpine meadow soils, which are generally alkaline, and rainwater scouring, or infiltration will lead to changes in groundwater pH. These indicators have the most prominent impact on water quality. The source region of the Yellow River is an ecologically sensitive area, mainly due to animal husbandry, with a single industrial structure, so some toxicological indicators are not considered. In 2016–2020, groundwater was collected from different monitoring points using 500mL polyethylene bottles. The collected water samples were transported to the laboratory of Qinghai University within 24 h. The temperature and pH of groundwater were measured on site. Total hardness (Th), sulfate, consumption of oxygen (COD_{Mn}), total nitrogen (TN), total phosphorus (TP) and ammonia nitrogen were determined in accordance with the “China Environmental Protection Standards Collection: Water Quality Analysis Method” in the laboratory. The measurement items and methods are shown in Table 2.

Table 2. Determination items and methods.

Monitoring Items	Determined Methods
temperature	Merck 3401 portable multi-parameter tester (WTW)
pH	Merck 3401 portable multi-parameter tester (WTW)
total hardness/(mg/L)	EDTA titration: Under pH = 10, disodium ethylenediamine tetraacetate (EDTA) reacts with calcium and magnesium ions in water to form a stable complex, and the indicator chrome black T can also form a wine-red complex with calcium and magnesium ions, and it is not as stable as that formed by EDTA with calcium and magnesium ions. When the titration is close to the end point, EDTA takes calcium and magnesium ions from the wine-red complex of chromium black T to make the chrome black T indicator free, and the solution changes from wine-red to blue.
ammonia nitrogen/(mg/L)	Na’s reagent spectrophotometry: Ammonia nitrogen in the form of free ammonia or ammonium ions reacts with Nessler’s reagent to form a light reddish-brown complex. The absorbance of the complex is directly proportional to the ammonia nitrogen content, and the absorbance is measured at the wavelength of 420 nm.
sulfate/(mg/L)	Sulfate gravimetric method: Sulfate forms barium sulfate precipitation with added barium chloride in hydrochloric acid solution. Precipitate at a temperature close to boiling; boil for at least 20min; filter after aging the precipitate; and wash the precipitate until there is no chloride ion. Dry or burn the precipitate, and weigh the barium sulfate after cooling.
oxygen consumption/(mg/L)	Acid potassium permanganate titration: Use potassium permanganate as oxidant. This oxidizes reducing substances in water under certain conditions, and the amount of potassium permanganate consumed can be calculated to represent oxygen consumption.
TN/(mg/L)	Determination of TN through basic potassium persulfate–UV spectrophotometric method
TP/(mg/L)	Determination of TP through ammonium molybdate spectrophotometry

2021~2100, statistical downscale climate information on the CMIP5 global climate model for the period obtained by the IPCC Data Centre.

2.3. Evaluation Method of Groundwater Quality

Single-component evaluation method: According to the classification indexes listed in the “Groundwater Quality Standard” (No. GB/T14848-2017), the water quality index content of the monitoring points was compared with the Chinese national evaluation standards to classify the categories to which their water quality indexes belonged [38]. The evaluation criteria are shown in Table 3.

Table 3. Quality standard for groundwater.

Index \ Category	I	II	III	IV	V
pH		6.5 ≤ pH ≤ 8.5		5.5 ≤ pH < 6.5 8.5 < pH ≤ 9.0	pH < 5.5 or pH > 9.0
Total hardness/(mg/L)	≤150	≤300	≤450	≤650	>650
Oxygen consumption/(mg/L)	≤1.0	≤2.0	≤3.0	≤10.0	>10.0
Sulfate/(mg/L)	≤50	≤150	≤250	≤350	>350
Ammonia nitrogen/(mg/L)	≤0.02	≤0.10	≤0.50	≤1.50	>1.50

Comprehensive evaluation method: This study adopted the adding scoring method in the comprehensive evaluation method. Firstly, after the evaluation of the individual components of the water quality indicators, the components were classified into the categories shown in Table 4 and the evaluation score F_i of each individual component was determined [39].

Table 4. Individual component evaluation F_i .

Category	I	II	III	IV	V
F_i	0	1	3	6	10

Secondly, the score of comprehensive evaluation (F) was calculated as follows:

$$F = \frac{\sqrt{\bar{F}^2 - F_{\max}^2}}{2} \quad (1)$$

$$\bar{F} = \frac{1}{n} \sum_{i=1}^n F_i \quad (2)$$

where: F —the composite evaluation score;

\bar{F} —the average of the individual component evaluation scores for F_i ;

F_{\max} —the maximum of the mean individual component score in F_i ;

n —number of items.

Finally, the groundwater quality class in the source region of the Yellow River is classified according to the composite price tag score F (Table 5).

Table 5. Comprehensive evaluation of groundwater quality.

Water Quality Level	Excellent	Good	Not Bad	Poor	Very Poor
F	<0.80	0.80–2.50	2.50–4.25	4.25–7.20	>7.20

2.4. Methods for Groundwater Quality Prediction

Construction of SWAT model database: The soil database, meteorological database and groundwater runoff database were established, respectively, in the source region of the Yellow River.

The establishment of the SWAT model: The reprocessed DEM map was used to extract the groundwater runoff network, divide the sub-basins of the groundwater system in the source region of the Yellow River, calculate the overall parameters of the basin, overlay soil data, land use, land cover data and groundwater runoff data, and set the three thresholds to divide the hydrological response unit (HRU). Groundwater data collected and measured in the previous period were processed and employed to calibrate and verify the model parameters. When the SWAT program starts running, it indicates whether the SWAT model has been successfully created.

Parameter sensitivity analysis and calibration of SWAT model: We conducted a parameter analysis of runoff that adopted the self-contained module of the model, and the method of the module is the LH-OAT method. Through sensitivity analysis, soil bulk density (SOL-BD) and the SCS runoff curve number (CN2) were generated. Ten parameters related to groundwater runoff were used, such as soil evaporation compensation coefficient (ESCO), effective hydraulic conductivity of main riverbed (CH-K2), saturated water conductivity of soil layer (SOL-K), effective water capacity of soil layer (SOL-AWC), attenuation coefficient of base flow (ALPHA-BF), threshold of water storage in shallow aquifer (GWQMN), compensation coefficient of plant absorption (EPCO), critical water holding capacity of shallow water (REVAPMN), etc. We used SWAT software to calibrate the parameters and find the optimal parameter values. The value of the optimal parameter was obtained using SWAT-CUP itself, and the final value range of the parameter was defined. Being dependent on the value range of the parameter calibration, the parameter range was continuously reduced through iterative analysis, and finally the optimal solution was obtained, that is, the rating value of the input model. According to the results of the above analysis, the absolute rate of each datum is within the range of the value obtained, and the stimulation effect is better. The optimal parameter values were input into the SWAT model to preheat, verify, and compare the actual measured values of the model.

Verification of SWAT model: The model rate is from 2000 to 2013, and the verification period is from 2014 to 2018. The deviation between the simulation value of the rate period and the verification period and the actual measurement data observed by the groundwater observation point is within 10%. Periodic NSE is 0.876 and the verification period NSE is 0.972 (Figure 2). These suggest that the model has strong applicability and high reliability in the source region of the Yellow River.

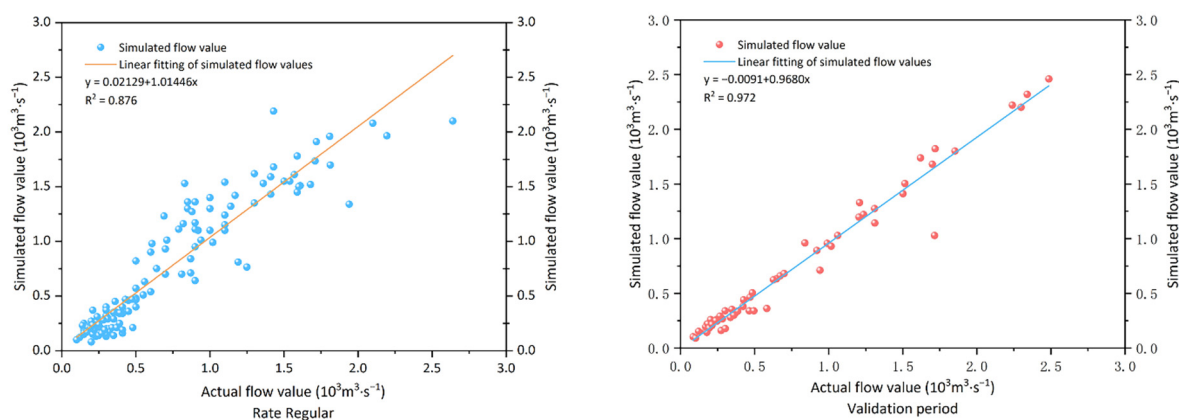


Figure 2. Scatterplot of simulated and measured monthly runoff values in the source region of the Yellow River.

Coupling of CMIP5 global climate model and SWAT hydrological model: Using the Future Scenario Prediction Dataset produced by the China Climate Center, the dataset is made up of the simulation results of 21 CMIP5 global climate models. A total of 21 climate models are shown in Table 6. After carrying out interpolation calculations to unify and downscale them to the same resolution (Peng et al. 2018), a multi-model ensemble was produced using the simple averaging method to produce a set including 1901~2005 historical and 2006~2100 monthly averages for RCP2.6, RCP4.5, and RCP8.5 emission scenarios in the source region of the Yellow River. The data were then input into the SWAT model, and the output results were downscaled using the statistical downscaling method by driving the ratified and validated SWAT model. The processed meteorological results and the collected spatial, soil, hydrological and water quality data of the source area were used as the initial data of the ratified SWAT hydrological model, which were imported into the model, and then the output predictions were obtained. The data of groundwater quality in

the source region of the Yellow River from 2021 to 2100 will be used to simulate the trend of groundwater quality in the source region of the Yellow River.

Table 6. The basic information about 21 CMIP5 global climate model.

Model	Research institution	Resolution
Beijing Climate Center Climate System Model version 1 (BCC-CSM1-1)	BBC, China Meteorological Administration, China	128 × 64
Beijing Normal University Earth System Model (BNU-ESM)	The College of Global Change and Earth System Science (GCESS), BNU, China	128 × 64
Canadian Earth System Model version 2 (CanESM2)	Canadian Centre for Climate Modelling and Analysis, Canada	128 × 64
The Community Climate System Model version 4 (CCSM4)	National Center for Atmospheric Research, USA	288 × 192
Centre National de Recherches Meteorologiques Climate Model version 5 (CNRM-CM5)	CNRM/Centre Europeen de Recherche et Formation Avancees en Calcul Scientifique, France	256 × 128
Commonwealth Scientific and Industrial Research Organization Mark Climate Model version 3.6 (CSIRO-MK3-6-0)	CSIRO in collaboration with Queensland Climate Change Centre of Excellence, Australia	192 × 96
Flexible Global Ocean- Atmosphere-Land System Model-grid version 2 (FGOALS-g2)	State Key Laboratory of Numerical Modeling for Atmospheric Sciences and Geophysical Fluid Dynamics, Institute of Atmospheric Physics, Chinese Academy of Sciences, and Tsinghua University, China	128 × 60
The First Institution of Oceanography Earth System Model (FIO-ESM)	FIO, State Oceanic Administration (SOA), Qingdao, China	128 × 64
Geophysical Fluid Dynamics Laboratory Climate Model version 3 (GFDL-CM3)	GFDL, National Oceanic and Atmospheric Administration, USA	144 × 90
Geophysical Fluid Dynamics Laboratory Earth System Model version 2 with Generalized Ocean Layer Dynamics(GOLD) code base (GFDL-ESM2G)	GFDL, National Oceanic and Atmospheric Administration, USA	144 × 90
Geophysical Fluid Dynamics Laboratory Earth System Model version 2 with Modular Ocean Model version 4.1 (GFDL-ESM2M)	GFDL, National Oceanic and Atmospheric Administration, USA	144 × 90
Goddard Institute for Space Studies Model E version 2 with Hycoml ocean model (GISS-E2-H)	GISS, National Aeronautics and Space Administration, USA	144 × 90
Goddard Institute for Space Studies Model E version 2 with Russell ocean model (GISS-E2-R)	GISS, National Aeronautics and Space Administration, USA	144 × 90
the Met Office Hadley Centre Global Environment Models version 2 with the new atmosphere-ocean component model (HadGEM2-AO)	Jointly with Met Office Hadley Centre and National Institute of Meteorological Research (NIMR), Korea Meteorological Administration (KMA), Seoul, South Korea	192 × 145
Institut Pierre Simon Laplace Climate Model 5A-Low Resolution (IPSL-CM5A-LR)	IPSL, France	96 × 96
Model for Interdisciplinary Research on Climate-Earth System, version 5 (MIROC5)	Atmosphere and Ocean Research Institute(AORI), National Institute for Environmental Studies (NIES) Japan Agency for Marine-Earth Science and Technology, Kanagawa (JAMSTEC), Japan	256 × 128
Model for Interdisciplinary Research on Climate-Earth System (MIROC-ESM)	JAMSTEC, AORI, and NIES, Japan	128 × 64
Atmospheric Chemistry Coupled Version of Model for Interdisciplinary Research on Climate-Earth System(MIROC-ESM-CHEM)	JAMSTEC, AORI, and NIES, Japan	128 × 64
Max-Planck Institute Earth System Model-Low Resolution (MPI-ESM-LR)	MPI for Meteorology, Germany	192 × 96
Meteorological Research Institute Coupled General Circulation Model version 3 (MRI-CGCM3)	MRI, Japan	320 × 160
The Norwegian Earth System Model version I with Intermediate Resolution(NorESM1-M)	Norwegian Climate Centre, Norway	144 × 96

Fitting of simulation results using the linear trend method: A one-dimensional linear regression equation between the two variables was established using x_i to represent a climate variable with a sample size of n and t_i to represent the corresponding time (Li et al. 2016).

$$\hat{x}_i = a + bt_i, i = 1, 2, \dots, n \quad (3)$$

where a represents the regression constants and b the regression coefficients (propensity values). $b \times 10$ represents the climate propensity ratios. The sign of b can be used to determine the tendency of the climate variable to change, and the absolute value can be used to reflect the rate of change of the climate variable.

2.5. Data Processing

Trend analysis of water temperature, pH, total hardness, oxygen consumption (COD_{Mn}), sulfate, and ammonia nitrogen interannual variation data at different monitoring points in the source region of the Yellow River from 2016 to 2020 and trend prediction analysis of changes in TN and TP contents in groundwater under three future scenarios in the source area by the software of Origin 2021 and Excel 2016.

The overall experimental flowchart is shown in Figure 3.

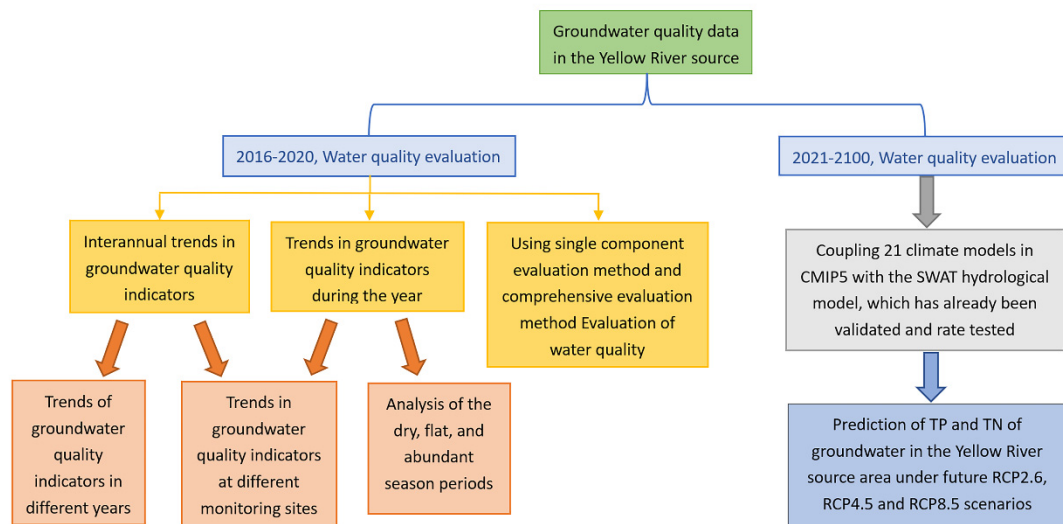


Figure 3. Flowchart.

3. Results

3.1. Analysis of Interannual Variation in Groundwater in the Source Region of the Yellow River

Figure 4A shows the first groundwater area at Tong De junction of 101 provincial highway. There is an overall increasing trend in temperature, total hardness (Th), sulfate, oxygen consumption (COD_{Mn}), and ammonia nitrogen levels from 2016 to 2020. An overall increasing trend was found for temperature, Th, sulfate, and NH_4^+ -N levels. The maximum values of Th, COD_{Mn} and NH_4^+ -N were observed in 2019. The interannual variation in pH decreased and groundwater was generally weakly alkaline. The water quality in the area was slightly worse in 2019 compared to other years. For the second groundwater area at Tong De junction of 101 provincial highway (Figure 4B), the temperature, pH, COD_{Mn} , and NH_4^+ -N showed a clear upward trend. Th and sulfate fluctuated over five years, but there was no obvious trend of change. For the first groundwater area at the head of LuanShitou, the values of temperature, pH, COD_{Mn} , and NH_4^+ -N showed significant interannual variations and substantial increases. Temperature, COD_{Mn} , and NH_4^+ -N were at their highest in 2020—10.41 °C, 1.245 mg/L, and 0.026 mg/L, respectively (Figure 4C). The interannual variation of the temperature and pH of the groundwater at the mouth of the second groundwater area at the head of LuanShitou showed an increasing trend,

with the temperature reaching the maximum value of 9.73 °C in 2020, while the rest of the indexes decreased, with the sulfate content showing a smaller decreasing trend (Figure 4D). The groundwater quality indicators of Laodeang Township had increasing interannual change indicators—temperature, pH and NH₄⁺-N, with both temperature and pH having maximum values in 2020. The water quality indicators that decreased are Th, COD_{Mn} and sulfate, with the minimum values of Th and sulfate, respectively, being 138.92 mg/L and 15.44 mg/L in 2020 (Figure 4E). The temperature, pH, and Th of the groundwater in WoSai township increased significantly from 2016 to 2020. Temperature and Th were at their maximum in 2020, at 10.11 °C and 155.35 mg/L, respectively. The values of COD_{Mn} and NH₄⁺-N showed decreasing trends (Figure 4F). The groundwater in the southern part of XingXinghai river had significant interannual variations in temperature, pH, Th and NH₄⁺-N. The maximum temperature in 2020 was 9.66 °C, and the minimum temperature in 2016 was 8.85 °C. The maximum pH value was 7.78 in 2017, maximum Th value was 172.16 mg/L in 2019, and the lowest value was 139.21 mg/L in 2017. While there was a clear trend of interannual variation in sulfate, COD_{Mn} levels showed a decreasing trend over the five years of water quality monitoring and were at their minimum value in 2019 (Figure 4G).

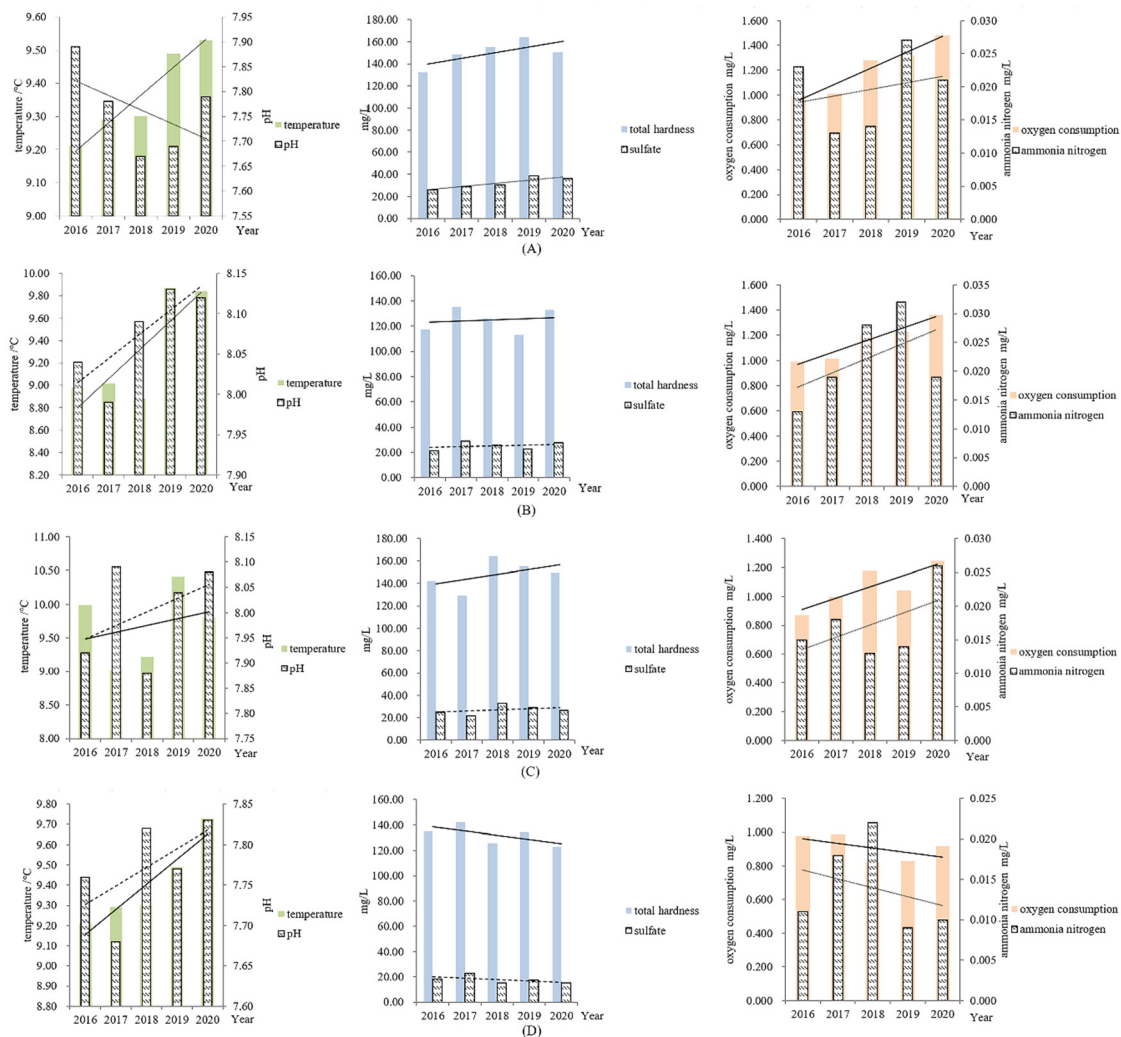


Figure 4. Cont.

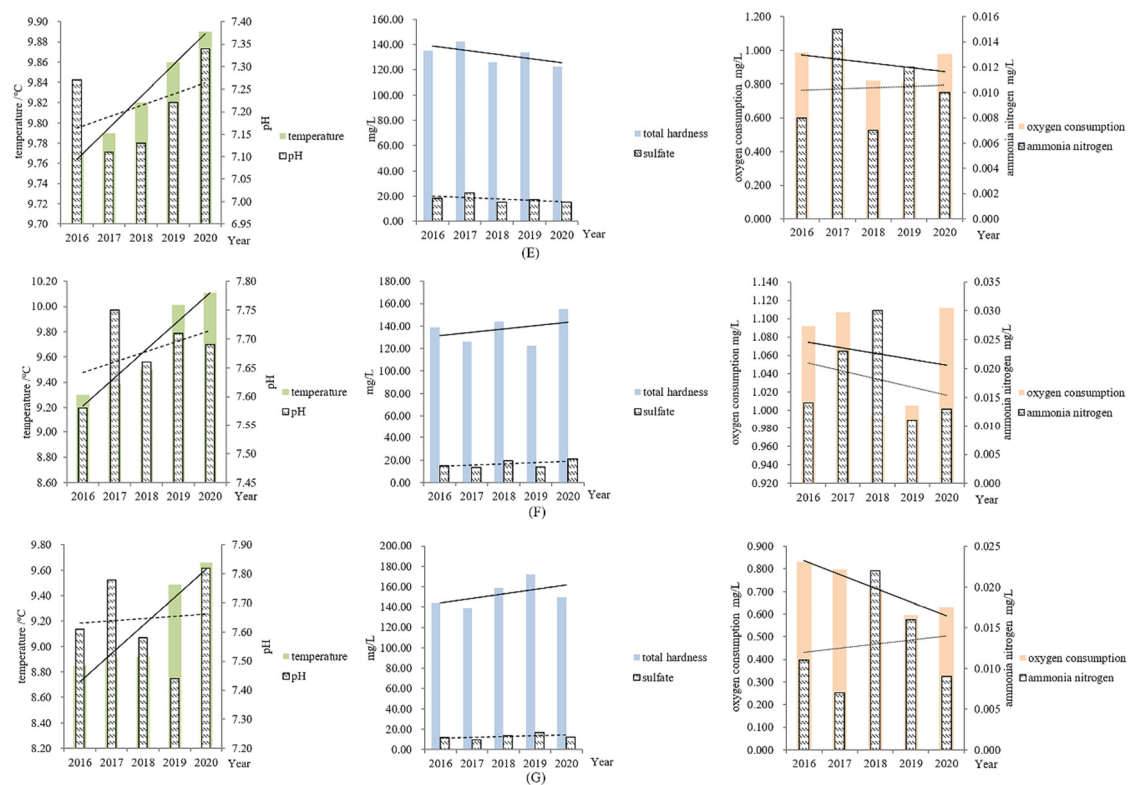


Figure 4. Interannual variation of different water quality indicators at different monitoring points of groundwater in the source region of the Yellow River. (A) Interannual variation of the first groundwater area under different water quality indexes at TongDe junction of 101 provincial highway. (B) Interannual variation of the second different water quality indexes in groundwater at TongDe junction of 101 provincial highway. (C) Interannual variation of the first groundwater area under different water quality indexes at the head of LuanShitou. (D) Interannual variation of the second groundwater area under different water quality indexes at the head of LuanShitou (at 845 km along 101 provincial highway). (E) Interannual variation of different water quality indexes of groundwater in LaoDeang township (at 636 km of 101 provincial highway). (F) Interannual variation of groundwater quality indexes in WoSai township (23 km from DaRi county). (G) Interannual variation of different water quality indicators of groundwater in the southern part of Xingxinghai River (at 508 km along 214 National Highway).

According to Figure 5, the interannual temperature, $\text{NH}_4^+\text{-N}$ and COD_{Mn} significantly increased. The highest temperature was 9.80 °C in 2019, and the lowest temperature was 9.39 °C in 2016. The maximum $\text{NH}_4^+\text{-N}$ content was 0.019 mg/L in 2018, and the minimum value was 0.014 mg/L in 2016. COD_{Mn} reached its maximum in 2020. pH had a clear downward trend over the 5 years, of which the smallest value was 8.07 in 2020. The Th and sulfate levels fluctuated overall, but there was no obvious increasing or decreasing trend.

3.2. Analysis of Intraannual Variation of Groundwater in the Source Region of the Yellow River

The changes in groundwater quality indicators in 2016~2020 at the first groundwater monitoring point of Tong De junction of 101 provincial highway. Temperature and COD_{Mn} were at their largest in the abundant season and the smallest in the dry season. The Th and $\text{NH}_4^+\text{-N}$ change trends were opposite to this, with minimum values in the abundant season. pH was at its largest in the flat season (Figure 6A). The temperature and COD_{Mn} of groundwater at the second groundwater monitoring point of Tong De junction of 101 provincial highway increased with the water volume. pH and $\text{NH}_4^+\text{-N}$ contents changed in opposite trends (Figure 6B). Figure 6C show that the first groundwater area at the head of the Luan-Shitou monitoring point within the year changes, and that the temperature and COD_{Mn}

content increased with the increase in water volume. $\text{NH}_4^+\text{-N}$ content decreased with increasing water volume. According to Figure 6D, the values of temperature, COD_{Mn} and sulfate at the second groundwater area at the head of LuanShitou were at their the largest in the abundant season and smallest in the dry season. pH and $\text{NH}_4^+\text{-N}$ were at their smallest in the abundant season and largest in the dry season. There was a tendency for temperature, COD_{Mn} in the groundwater at LaoDeang township to become larger as the amount of groundwater increases. $\text{NH}_4^+\text{-N}$ changed in the opposite trend (Figure 6E). The groundwater in WoSai township in temperature and $\text{NH}_4^+\text{-N}$ indicated in the monitoring of the conditions of abundant season > flat season > dry season, sulfate and COD_{Mn} in the conditions of abundant season < flat season < dry season. pH had a maximum value of 7.80 in the abundant season (Figure 6F). In the southern part of XingXing river, groundwater temperature and COD_{Mn} content had a pattern of increasing with the increase in water volume; the change in $\text{NH}_4^+\text{-N}$ content showed the opposite trend (Figure 6G).

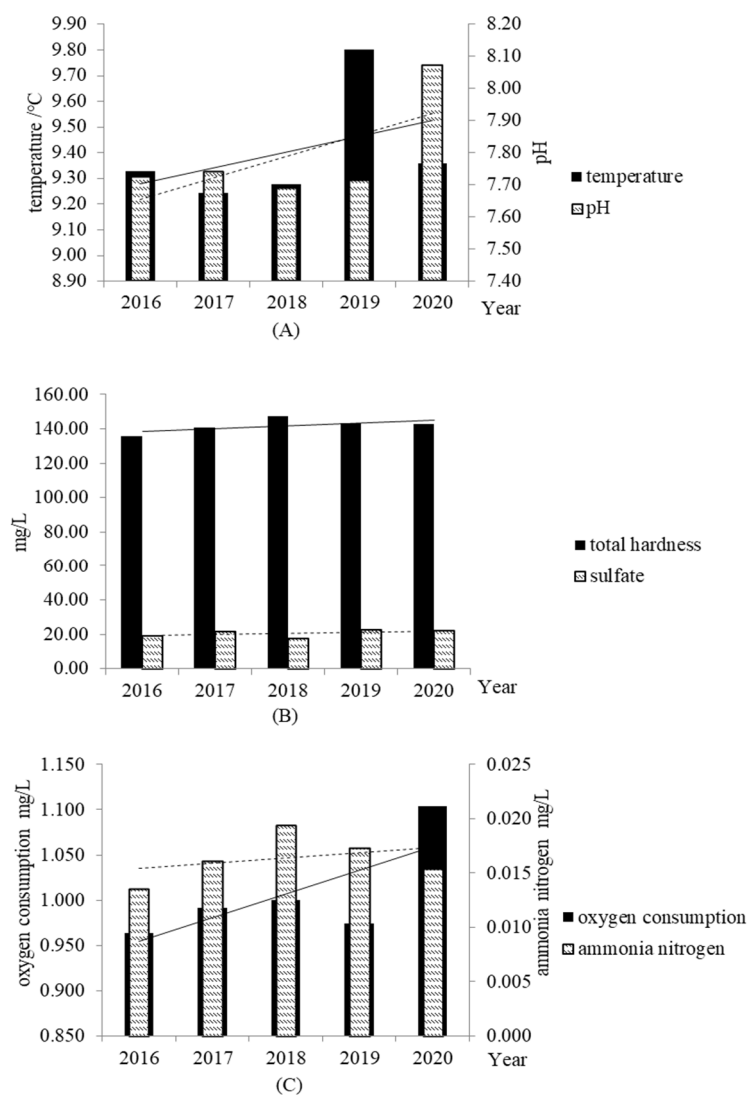


Figure 5. Interannual variation of groundwater in the source region of the Yellow River. (A) Temperature and pH. (B) Total hardness and sulfate. (C) Ammonia nitrogen and oxygen consumption.

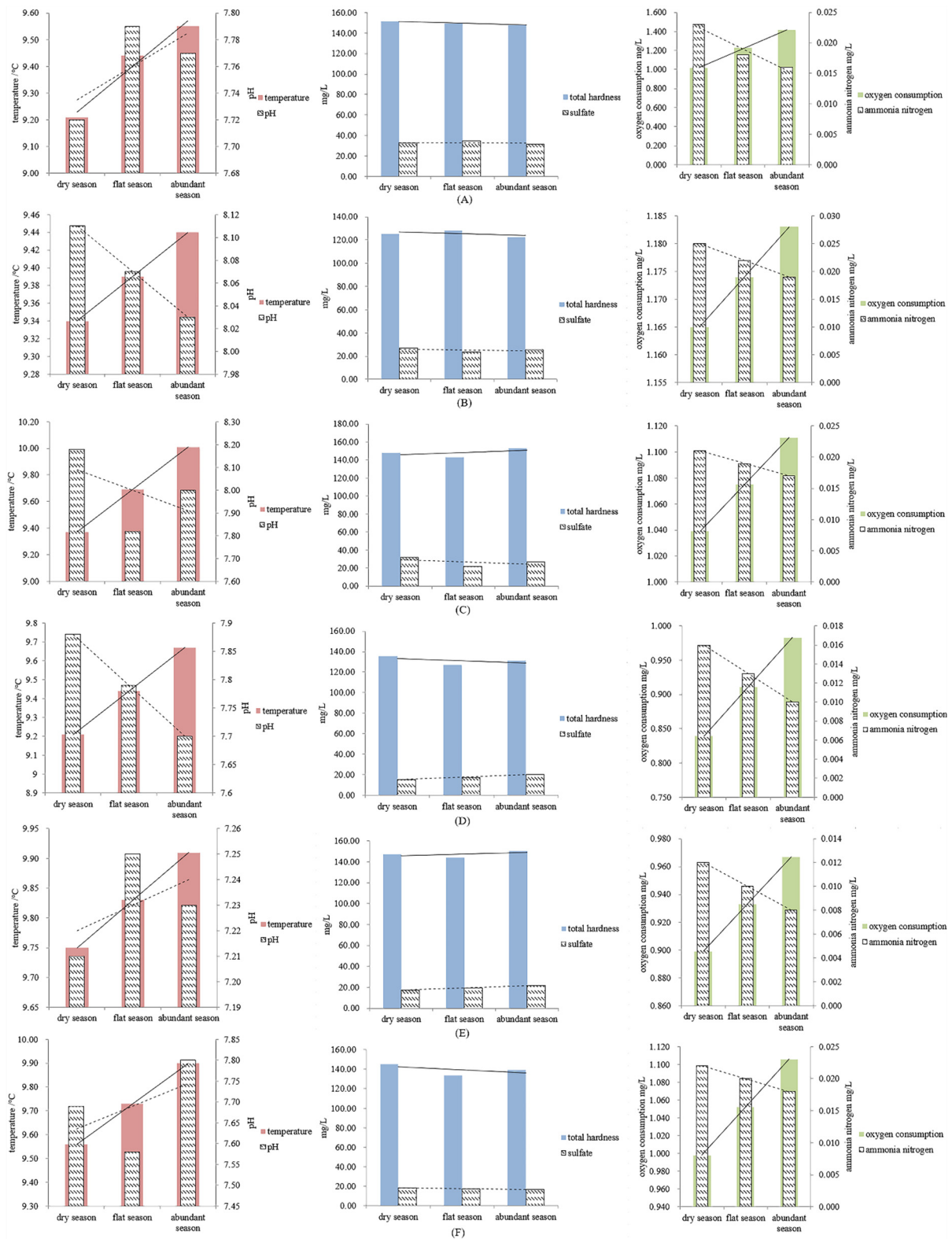


Figure 6. Cont.

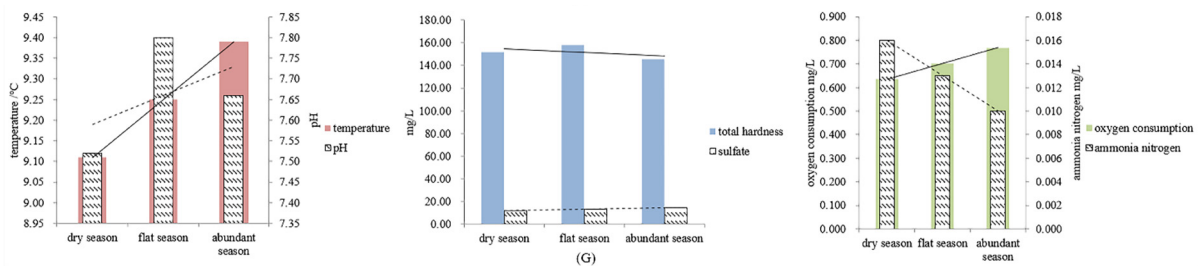


Figure 6. Annual variation in different indicators of groundwater at different monitoring points in the source region of the Yellow River. (A) Annual variation of the first groundwater at TongDe junction of 101 provincial highway. (B) Annual variation of the second groundwater at TongDe junction of 101 provincial highway. (C) Annual variation of the first groundwater at the head of Luan Shitou. (D) Annual variation of the second groundwater at the head of LuanShitou (845 km along 101 provincial highway). (E) Annual variation of groundwater in LaoDeang township (636 km along 101 provincial highway). (F) Annual variation of groundwater in WoSai township (23 km from DaRi county). (G) Annual variation of groundwater in the southern part of Xingxinghai River (508 km along 214 National Highway).

According to Figure 7, the groundwater temperature and COD_{Mn} in the source region of the Yellow River all had the relationship of abundant season > flat season > dry season and $\text{NH}_4^+\text{-N}$ had the relationship of abundant season < flat season < dry season, while Th and sulfate had different relationships in different periods. Therefore, the Th and sulfate of the groundwater have no obvious relationship with different periods of the year.

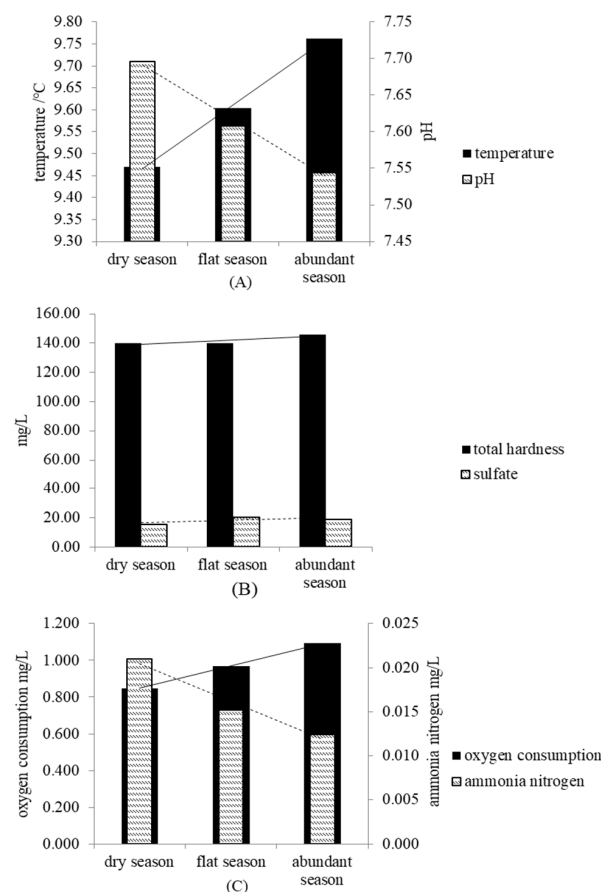


Figure 7. Annual variation of groundwater in the source region of the Yellow River. (A) Temperature and pH. (B) Total hardness and sulfate variation. (C) Ammonia nitrogen and oxygen consumption.

3.3. Analysis of Single-Component Evaluation Method Evaluation Results

The groundwater quality from 2016 to 2020 can be seen in Table 7. The water quality indicators except COD_{Mn} were up to the Class I water quality specified in the “Standards of Groundwater Quality” (No. GB/T14848-2017). COD_{Mn} reached the class I standard from 2016 to 2019, but the COD_{Mn} content increased, and the water quality deteriorated in 2020, and COD_{Mn} content reached the class II standard.

Table 7. Results of the evaluation of groundwater in the source region of the Yellow River.

Index	Year	2016	2017	2018	2019	2020
	pH		I	I	I	I
Total hardness/(mg/L)		I	I	I	I	I
Oxygen consumption/(mg/L)		I	I	I	I	II
Sulfate/(mg/L)		I	I	I	I	I
Ammonia nitrogen/(mg/L)		I	I	I	I	I

3.4. Analysis of Comprehensive Evaluation Method Evaluation Results

The comprehensive evaluation method of groundwater quality was based on the individual indicators, compensating for the single-factor evaluation. The groundwater quality status was classed as “Excellent” from 2016 to 2020. However, according to the magnitude of the comprehensive score value F, the F value was 0.00 from 2016 to 2019, but the F value was 0.72 in 2020. It can be seen in Table 8 that the larger the F value, the worse the water quality. This shows that the groundwater quality deteriorated in 2020 in the source region of the Yellow River.

Table 8. Results of the comprehensive evaluation of groundwater in the source region of the Yellow River.

Year	Integrated Rating F	Water Quality
2016	0.00	Good
2017	0.00	Good
2018	0.00	Good
2019	0.00	Good
2020	0.72	Good

3.5. Prediction of Groundwater Quality in the Source Region of the Yellow River

Under the three RCPs climate change scenarios, the interannual variation of TN and TP contents in the source region showed an increasing trend. The relationship between the simulated TN and TP increase rates under the three scenarios were all $\text{RCP 8.5} > \text{RCP 4.5} > \text{RCP 2.6}$, and the interannual difference in content among the three scenarios increases with the passage of time. According to Figure 8A, the future TN content had a small change, which is mainly characterized by interannual oscillations under the RCP 2.6 climate scenario. The future TN content was increased in the first and mid-century obviously and fluctuated less at the end under the RCP 4.5 climate scenario. Under the RCP 8.5 climate scenario, the future TN content showed obvious linear growth throughout the 21st century, and the fluctuations are relatively uniform. According to Figure 8B, the future TP content fluctuated greatly early on in the century and changed less at the end of century under the RCP 2.6 climate scenario. Under the RCP 4.5 climate scenario, the future TP content changed similarly to RCP 2.6. The future TP content of the source region was increased significantly in the early and late 21st century, and only slowly decreased in the middle of this century under the RCP 8.5 climate scenario.

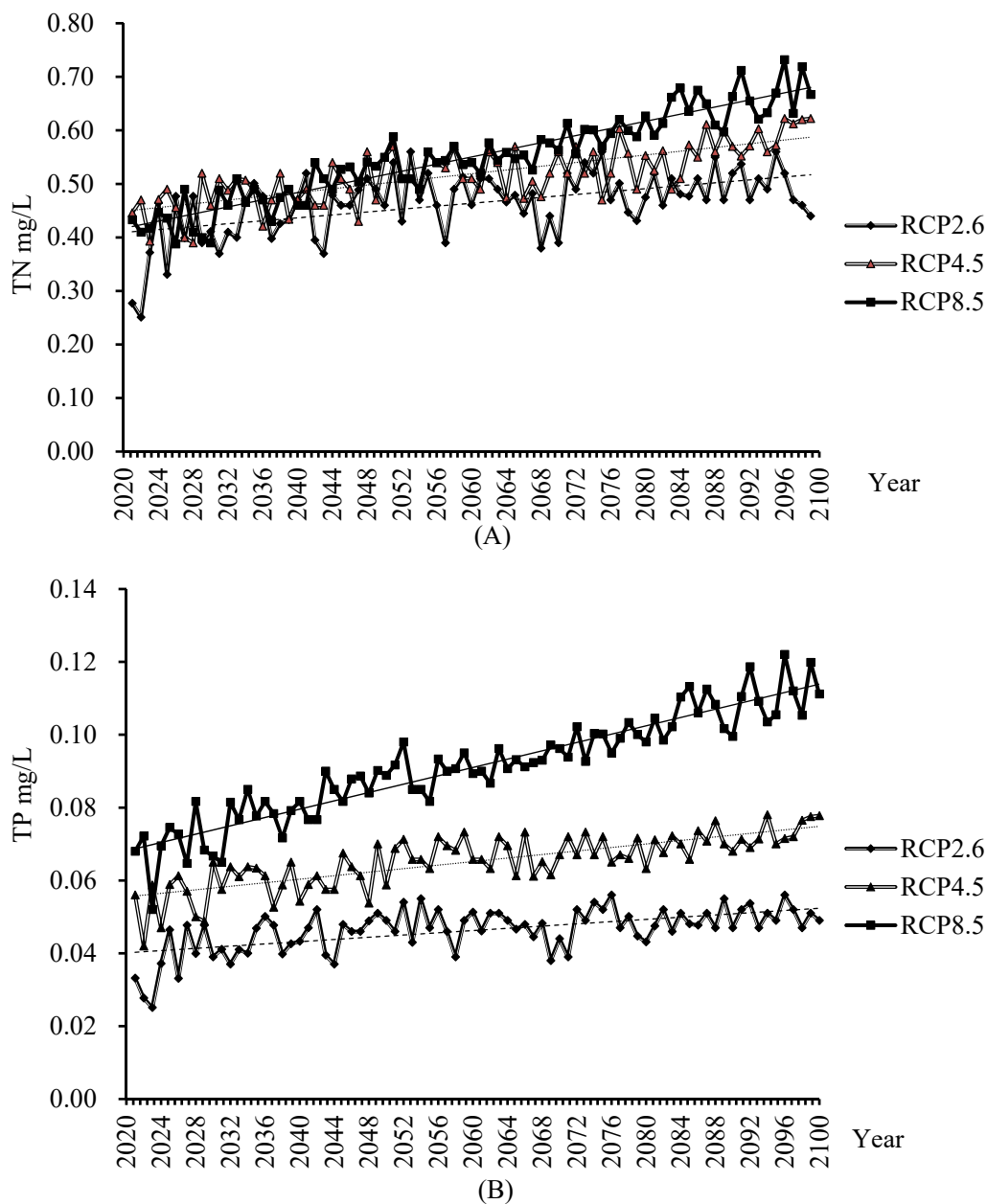


Figure 8. Interannual distribution of total nitrogen (TN) and total phosphorus (TP) in water under three scenarios. (A) Total nitrogen (TN). (B) Total phosphorus (TP).

4. Discussion

In this study, the groundwater quality was good in the source region of the Yellow River, and all water quality indicators met the Class I standard specified in the Groundwater Quality Standard, except for COD_{Mn} , and only COD_{Mn} was relatively high in 2019, reaching the Class II standard, which was similar the studies conducted by Cao et al. [40] and Shi et al. [41]. This is related to the slowing down of overgrazing, the reduction in livestock and poultry manure output, and the reduction in man-made pollution. This indicated that COD_{Mn} was the main source of pollutants in the groundwater in the source region. The COD_{Mn} content of groundwater in the source region of the Yellow River was higher in the abundant water period in the three periods. However, Yang Wanling et al. [42] evaluated the water bodies in the Pearl River Delta river network area (China). They concluded that COD_{Mn} was lower during the abundant water period compared to the other two periods, which may be due to the lower temperature of the groundwater in the source region of

the Yellow River during the dry season. Organic matter in water decomposes slowly, resulting in the timely oxidation of reducing substances in the water, and thus a lower content of COD_{Mn} in water [43]. The groundwater quality of different monitoring points is slightly different in the source region of the Yellow River: the groundwater at the head of LuanShitou, the groundwater at LaoDeang township and the groundwater in the southern part of XingXinghai river were slightly poorer than other sampling points, and the organic content increased, which may be related to the monitoring point being located near the highway; the exhaust gas and dust from vehicles have an impact on the groundwater. There are grasslands around the groundwater, which are severely degraded. There is also grazing, and so animal manure enters the groundwater under the washing of rainwater, causing groundwater pollution. Human activities are relatively frequent, and domestic sewage and garbage produced by human activities have an impact on groundwater and make groundwater quality worse, but this will require further study [44].

The chemical properties (temperature, turbidity, color, dissolved oxygen, pH, etc.) of groundwater are the basic parameters that determine the quality of groundwater, while water chemical characteristics (major ions and anions) are key factors in groundwater quality. Xia et al. [45] proposed carrying out a comprehensive evaluation of water quality according to the water demands of the ecological environment. Ankit N et al. [46] used a weighted arithmetic approach to evaluate the groundwater quality index, and concluded that the groundwater quality index (GWQI) was one of the most effective tools for evaluating groundwater quality, which uses the maximum values of various water quality variables to provide easily understandable results, while the comprehensive evaluation method used in this paper used the mean value calculation to obtain the final water quality criteria, so the influence of these two evaluation methods on the results of the final evaluation of water quality needs to be studied further in the future. Mehta D et al. [47] expressed the contribution of each indicator to water quality by calculating the groundwater quality index including the weighting factors of the specified groundwater quality parameters, the groundwater quality criteria, and the analytical concentrations of each water quality parameter, and we based this on the water quality in the single-component evaluation method to further calculate its comprehensive evaluation score. In this paper, different indicators (temperature, pH, Th, sulfate, COD_{Mn} , $\text{NH}_4^+\text{-N}$, TN and TP) of groundwater in the source area for five years from 2016 to 2020 were evaluated using the single-indicator evaluation method, but the influence of pollution indicators on water quality was overemphasized, so a comprehensive evaluation method was used to evaluate the groundwater quality in the source area for five years, and its evaluation was able to focus on the pollution indicators, involving the mean value of the evaluation indicators, and the evaluation was more scientific. The desired results were obtained, and the evaluation results were basically consistent with previous study [48].

This paper estimated the future (2021–2100) changes in TN and TP content by coupling the RCP 2.6, RCP 4.5 and RCP 8.5 (low emission, medium-low emission and high emission) climate scenarios under the CMIP5 model with the SWAT hydrological model in the source region of the Yellow River. This showed an overall upward trend. This is consistent with Liu Mei's study on the changing trend of total nitrogen and total phosphorus in eastern China [49]. This study used 21 models in CMIP5 to predict the changes in groundwater quality in the source region of the Yellow River. More models were adopted, which overcomes the shortcomings of using a single model or fewer models. The prediction results are more accurate and reliable. This provides scientific support for groundwater protection in the source region of the Yellow River under climate change. Shi constructed a distributed hydrological model and used the output of five GCMs to predict the change trend of water resources in the next 100 years in the source region of the Yellow River. We concluded that the runoff sensitivity is highly sensitive to precipitation, and can be used to obtain ideal results [50]. This study predicts the contents of TN and TP in groundwater under three future climate scenarios under the CMIP5 model by coupling the SWAT model, and satisfactory results were obtained. The previous research of our group found that

the regular NSE of the SWAT model rate was 0.876 in the source region of the Yellow River, and the NSE of the verification period was 0.972. Both of these were of good standard. The simulated total water volume of the SWAT model and the actual total water volume differed by -1.4% and 3.9% , respectively; the data difference is within a reasonable range, indicating that the SWAT model has strong applicability and high credibility in the source region of the Yellow River. The coupling of the climate model and the distributed hydrological model needs to be further investigated. The source region of the Yellow River is in the hinterland of the Qinghai–Tibet Plateau. Its altitude is more than 3000m, and it has good vegetation coverage and simple vegetation types, mainly animal husbandry, single industrial structure, underdeveloped productivity, and less impact by human activities. Thus, the climate change in the future may be the closest to the simulated scenario under RCPs2.6, which will require further study. The limitation of this paper is that the latest climate model CMIP6 coupled with the SWAT hydrological model was not used for this study. CMIP6 multi-model integration for climate and interannual variability improved the ability to simulate, according to previous comparisons; CMIP6's simulation prediction can significantly improve the spatial distribution of rainfall in wet and semi-humid areas [51]. The difference of the simulation prediction ability in semi-arid areas such as dry high-altitude cold areas are not significant [52]. However, the differences in predictions for high-altitude/cold regions relative to the latest more refined CMIP6 model are yet to be further developed. The prediction of groundwater quality indicators in this study only focuses on the TP and TN in the water body, and future predictions should be made for dissolved oxygen, sulfate, and ammonia nitrogen, etc. The groundwater in the area needs to be continuously sampled to verify the prediction results.

5. Concluding Remarks

In this paper, the interannual and annual variations of groundwater quality in the source region of the Yellow River from 2016 to 2020 were investigated, the water quality was evaluated, and the contents of TN and TP in the source area from 2021 to 2100 were predicted. The results showed that:

- (1) From 2016 to 2020, the groundwater temperature, ammonia nitrogen and dissolved oxygen in the source region of the Yellow River all showed an increasing trend, while pH showed an obvious decreasing trend. The total hardness and sulfate content fluctuated up and down, but there was no obvious increasing or decreasing trend. The interannual water temperature and COD_{Mn} showed the trend of wet season > normal season > dry season. The ammonia nitrogen appeared in wet season < normal season < dry season.
- (2) From 2016 to 2020, the groundwater quality was excellent, and all the water quality indexes reached Class II and above standards of the “Groundwater Environmental Quality Standards” (GB/T14848-2017). However, the water quality in 2020 showed a trend of deterioration, which indicated that COD_{Mn} was the main pollutant in the source region of the Yellow River.
- (3) Under the future climate scenario, the increase rates of total nitrogen and total phosphorus are RCP 8.5 > RCP 4.5 > RCP 2.6, and the nitrogen and phosphorus contents of groundwater in the source region of the Yellow River show a gradually increasing trend.
- (4) In the context of climate change, it is urgent to formulate a scientific and reasonable groundwater protection and utilization strategy.

Author Contributions: Conceptualization, Y.Y. and X.Q.; methodology, S.L.; software, L.Q.; validation, Z.L. and M.L.; formal analysis, B.Y. and Y.W.; resources, S.L.; data curation, C.J. and Y.Q.; writing—original draft preparation, J.S. and J.L. (Jianming Li); writing—review and editing, J.S. and J.L. (Jianming Li); visualization, J.L. (Jiajun Li); project administration, J.S. and S.L.; funding acquisition, J.S. and S.L. All authors have read and agreed to the published version of the manuscript.

Funding: Supported by the National Natural Science Funds Fund (No. 31760147) and the project of the QingHai Science & Technology Department (No. 2020-ZJ-763) (No. 2021-ZJ-926).

Conflicts of Interest: The authors declare no competing interests.

References

- Xia, T. International Groundwater Research Program and Development Strategy Overview. *Environ. Sci. Manag.* **2019**, *44*, 1–5.
- Famiglietti, J.S. The Global Groundwater Crisis. *Nat. Clim. Chang.* **2014**, *4*, 945–948. [[CrossRef](#)]
- Richey, A.S.; Thomas, B.F.; Lo, M.H.; Famiglietti, J.S.; Swenson, S.; Rodell, M. Uncertainty in Global Groundwater Storage Estimates in a Total Groundwater Stress Framework. *Water Resour. Res.* **2015**, *51*, 5198–5216. [[CrossRef](#)]
- Ren, Y.; Wang, H. Water Resources Crisis and the Development of Water Industry. *J. Shandong Univ. Sci. Technol. (Soc. Sci. Ed.)* **2001**, *4*, 48–51.
- Wang, C. Global Water Crisis and Ecological Utilization of Water Resources. *Ecol. Econ.* **2014**, *30*, 4–7.
- Zhu, L. *Research of Groundwater Pollution and Vulnerability in the City of Yulin and Its Surrounding Areas*; Northwest University: Xi'an, China, 2012.
- Babiker, I.S.; Mohamed, M.; Hiyama, T. Assessing Groundwater Quality Using GIS. *Water Resour. Manag.* **2007**, *21*, 699–715. [[CrossRef](#)]
- El Osta, M.; Masoud, M.; Ezzeldin, H. Assessment of the geochemical evolution of groundwater quality near the El Kharga Oasis, Egypt using NETPATH and water quality indices. *Environ. Earth Sci.* **2020**, *79*, 1–18. [[CrossRef](#)]
- El Osta, M.; Masoud, M.; Alqarawy, A.; Elsayed, S.; Gad, M. Groundwater Suitability for Drinking and Irrigation Using Water Quality Indices and Multivariate Modeling in Makkah Al-Mukarramah Province, Saudi Arabia. *Water* **2022**, *14*, 483. [[CrossRef](#)]
- Aghajari, M.; Mozayyan, M.; Mokarram, M.; Chekan, A.A. Relationship between Groundwater Quality and Distance to Fault Using Adaptive Neuro Fuzzy Inference System (ANFIS) and Geostatistical Methods (Case Study: North of Fars Province). *Spat. Inf. Res.* **2019**, *27*, 529–538. [[CrossRef](#)]
- Zarinmehr, H.; Tizro, A.T.; Fryar, A.E.; Pour, M.K.; Fasihi, R. Prediction of groundwater level variations based on gravity recovery and climate experiment (GRACE) satellite data and a time-series analysis: A case study in the Lake Urmia basin, Iran. *Environ. Earth Sci.* **2022**, *81*, 1–11. [[CrossRef](#)]
- Chen, A.F.; Feng, Q.; Zhang, J.K.; Li, Z.S.; Wang, G. A Review of Climate Change Scenarios for Impacts Process Study. *Geogr. Sci.* **2015**, *35*, 84–90.
- Zhai, Y.; Li, Y.; Xu, Y. Characteristics of Arid Climate Change in Northern China under RCPs Scenario. *Plateau Meteorol.* **2016**, *35*, 94–106.
- Yuan, Z.; Xu, H.; Ye, X. Discussion on the Accuracy of Medium and Long-Term Groundwater Quality Forecasts: Taking Xi'an as an example. *Hydrogeol. Eng. Geol.* **1996**, *23*, 8–10.
- Deng, J. *The Basic Method of Grey System*; Huazhong University of Science and Technology Press: Wuhan, China, 1987.
- Qin, D. China's Climate and Environment Evolution. *Civilization* **2005**, *12*, 10–11.
- Taylor, K.E.; Stouffer, R.J.; Meehl, G.A. An Overview of CMIP5 and the Experiment Design. *Bull. Am. Meteorol. Soc.* **2011**, *93*, 485–498.
- Van Vuuren, D.P.; Edmonds, J.; Kainuma, M.; Riahi, K.; Thomson, A.; Hibbard, K.; Hurtt, G.C.; Kram, T.; Krey, V.; Lamarque, J.F.; et al. The Representative Concentration Pathways: An Overview. *Clim. Chang.* **2011**, *109*, 5–31. [[CrossRef](#)]
- Li, Z.; Lan, M. Prediction and uncertainties of extreme precipitation over the Yangtze River valley in the early 21st century. *Acta Meteorol. Sci.* **2018**, *76*, 47–61.
- Han, L.; Han, Z.; Li, S. Projection of heavy rainfall events in the middle and lower reaches of the Yangtze River valley in the 21st century under different representative concentration pathways. *J. Atmos. Sci.* **2014**, *37*, 529–540.
- Yao, S.; Jiang, D.; Fan, G. Projection of Precipitation Seasonality over China. *Atmos. Sci.* **2018**, *42*, 1378–1392.
- Cheng, X. Prediction of spatio-temporal characteristics of temperature and precipitation over the upstream of the Yangtze River basin based on CMIP5 mode. *Hydropower Energy Sci.* **2019**, *37*, 13–16.
- Jin, H.; Qin, J.; Zhen, Q.; Dong, X.; Hao, Z. Future climate change prediction in the source region of Yangtze River based on integrated method. *Water Power* **2019**, *45*, 9–13.
- Wang, Z. Retrospect and Prospect of Distributed Hydrological Model. *Green Sci. Technol.* **2018**, *18*, 154–155.
- Meshesha, T.W.; Wang, J.; Melaku, N.D.; McClain, C.N. Modelling groundwater quality of the Athabasca River Basin in the subarctic region using a modified SWAT model. *Sci. Rep.* **2021**, *11*, 1–12. [[CrossRef](#)] [[PubMed](#)]
- Meshesha, T.W.; Wang, J.; Melaku, N.D. Modelling spatiotemporal patterns of water quality and its impacts on aquatic ecosystem in the cold climate region of Alberta, Canada. *J. Hydrol.* **2020**, *587*, 124952. [[CrossRef](#)]
- Luo, Y.; He, C.; Sophocleous, M.; Yin, Z.; Hongrui, R.; Ouyang, Z. Assessment of crop growth and soil water modules in SWAT2000 using extensive field experiment data in an irrigation district of the Yellow River Basin. *J. Hydrol.* **2008**, *352*, 139–156. [[CrossRef](#)]
- Guzman, J.A.; Moriasi, D.N.; Gowda, P.H.; Steiner, J.L.; Starks, P.J.; Arnold, J.G.; Srinivasan, R. A model integration framework for linking SWAT and MODFLOW. *Environ. Model. Softw.* **2015**, *73*, 103–116. [[CrossRef](#)]
- Wang, G.; Jin, J.; Bao, Z.; Liu, C.; Yan, X. Impact of Climate Change on Water Resources and Adaptation Strategies in the Main Grain Production Belt of the North China. *Chin. J. Eco-Agric.* **2014**, *22*, 898–903.
- Zhan, C.; Ning, L.; Zou, J.; Han, J. A Review on the Fully Coupled Atmosphere-hydrology simulations. *Acta Geogr. Sin.* **2018**, *73*, 893–905.

31. Song, X. *Effects on Climate Change and Human Activities on the Hydrological Processes of the Xilinhe River*; Inner Mongolia Agricultural University: Hohhot, China, 2016.
32. Zheng, W.; Yang, X.; Cheng, X.; Wang, Y.; Zhang, M. Prediction of Major Cycle change over Upper Yangtze River based on CMIP5 and VIC model. *Hydrology* **2018**, *38*, 48–53.
33. Wang, J.; Kumar Shrestha, N.; Aghajani Delavar, M.; Worku Meshesha, T.; Bhanja, S.N. Modelling watershed and river basin processes in cold climate regions: A review. *Water* **2021**, *13*, 518. [[CrossRef](#)]
34. Meshesha, T.W.; Wang, J.; Melaku, N.D. A modified hydrological model for assessing effect of pH on fate and transport of Escherichia coli in the Athabasca River basin. *J. Hydrol.* **2020**, *582*, 124513. [[CrossRef](#)]
35. Zhang, S.; Li, Y. Decline in regional Groundwater Level and Related Environment Problems in the Head Water Area of the Yellow River. *Hydrogeol. Eng. Geol.* **2009**, *6*, 109–113.
36. Wang, J.; Li, J.; Zhang, R. Generation Method of Climate Scene Based in the Headwater Regions of the Yellow River. *Yellow River* **2012**, *34*, 35–37.
37. Mo, X.; Liu, S.; Hu, S. Co-evolution of climate-vegetation-hydrology and its mechanisms in the source region of Yellow River. *Acta Geogr. Sin.* **2022**, *77*, 1730–1744.
38. Zhou, M. Application and comparative study of several evaluation methods for water quality in surface water evaluation. *Water Resour. Dev. Manag.* **2022**, *8*, 50–55.
39. Zhuang, F.; Guo, Z.; Zhao, H. Evaluation of shallow groundwater quality in Liaocheng City and suggested countermeasures. *Shandong Water Resour.* **2022**, *9*, 54–55.
40. Cao, X.; Liu, H. Quality Analysis of Groundwater in Ningxia. *Ningxia Eng. Technol.* **2004**, *3*, 385–388.
41. Shi, L.; Zhao, X.; Ni, T.; Yang, Y.; Dou, X.; Han, D.; Bai, Z. Surface water quality in the source area of the Yellow River from the three Rivers in Qinghai Province. *Guizhou Agric. Sci.* **2012**, *40*, 220–223.
42. Yang, W.; Lai, Z.; Zeng, Y.; Shuai, F.; Li, H.; Wang, C. Spatial-temporal characteristics of CODMn in Surface Water of Middle and Downstream of the Pearl River and Water Environment Evaluations. *Acta Eco-Environ. Sci.* **2017**, *45*, 643–648.
43. Liu, Q.; Lai, Z.; Li, Y. Dynamic Patterns of the Permanganate Index from 2017 to 2018 in Surface Waters of the Mainstream of the Xijiang River of Water Environmental Evaluations. *J. Fish. Sci.* **2019**, *13*, 1194–1204.
44. Li, Y.; Dou, B.; Chen, Z. Study on Evaluation and Prediction Methods of Groundwater Quality. *Land Resour. Shandong* **2015**, *31*, 33–36.
45. Xia, X.; Yang, Z.; Wu, Y. Incorporating Eco-environmental Water Requirements in Integrated Evaluation of Water Quality and Quantity—A Study for the Yellow River. *Water Resour. Manag.* **2009**, *23*, 1067–1079. [[CrossRef](#)]
46. Chaudhari, A.N.; Mehta, D.J.; Sharma, N.D. Coupled effect of seawater intrusion on groundwater quality: Study of South-West zone of Surat city. *Water Supply* **2022**, *22*, 1716–1734. [[CrossRef](#)]
47. Mehta, D.; Chauhan, P.; Prajapati, K. Assessment of ground water quality index status in Surat City. In Proceedings of the Next Frontiers in Civil Engineering: Sustainable and Resilient Infrastructure, Mumbai, India, 30 November–1 December 2018.
48. Xu, C.; Tang, S.; Huang, J. Analysis on Evaluation and Pollution of Groundwater Quality in the Shallow Aquifer of Henan Section in the Lower Reaches of Huang River. *Groundwater* **2009**, *31*, 97–101.
49. Liu, M. *Simulation and Prediction of Climate Change in Eastern China and Assessment of the Response of Hydrology and Water Quality in a Typical Watershed*; Zhejiang University: Zhejiang, China, 2015.
50. Shi, Y. *Climate Change in the Head Regions of the Yellow River and Its Effects on Water Resources*; Hohai University: Nanjing, China, 2006.
51. Almazroui, M.; Saeed, F.; Saeed, S.; Ismail, M.; Ehsan, M.A.; Islam, M.N.; Abid, M.A.; O'Brien, E.; Kamil, S.; Rashid, I.U.; et al. Projected changes in climate extremes using CMIP6 simulations over SREX regions. *Earth Syst. Environ.* **2021**, *5*, 481–497. [[CrossRef](#)]
52. Almazroui, M.; Saeed, F.; Saeed, S.; Nazrul Islam, M.; Ismail, M.; Klutse, N.A.B.; Siddiqui, M.H. Projected change in temperature and precipitation over Africa from CMIP6. *Earth Syst. Environ.* **2020**, *4*, 455–475. [[CrossRef](#)]